PHYSICAL REVIEW APPLIED 2, 061001 (2014)

Nonlinear Behavior and Mode Coupling in Spin-Transfer Nano-Oscillators

Romain Lebrun, Nicolas Locatelli, Sumito Tsunegi, Julie Grollier, and Vincent Cros*
Unité Mixte de Physique CNRS/Thales, Palaiseau and Université Paris-Sud, Orsay, France

Flavio Abreu Araujo
Institute of Condensed Matter and Nanosciences, Université catholique de Louvain, Louvain-la-Neuve, Belgium

Hitoshi Kubota, Kay Yakushiji, Akio Fukushima, and Shinji Yuasa
National Institute of Advanced Industrial Science and Technology (AIST), Spintronics Research Center, Tsukuba, Japan

(Received 28 July 2014; revised manuscript received 22 October 2014; published 8 December 2014)

By investigating thoroughly the tunable behavior of coupled modes, we highlight how it provides a means to tune the properties of spin-transfer nano-oscillators. We first demonstrate that the main features of the microwave signal associated with coupled vortex dynamics, i.e., frequency, spectral coherence, critical current, and mode localization, depend drastically on the relative vortex core polarities. Second, we report a large reduction of the nonlinear linewidth broadening obtained by changing the effective damping through the control of the core configuration. Such a level of control on the nonlinear behavior reinforces our choice to exploit the microwave properties of collective modes for applications in advanced spintronics devices for integrated telecommunication concerns.

DOI: 10.1103/PhysRevApplied.2.061001

Spin-transfer torque reveals the potential of spintronics devices for a new generation of electronic components showing multiple functionalities [1,2], notably for microwave applications [3]. Within this palette of new applications, spin-transfer nano-oscillators (STNOs) relying on the conversion of nonlinear magnetization dynamics into a microwave signal are anticipated as being the most promising one, given their high spectral coherence [4,5], large tunability with current [3], frequency modulation properties [6,7], and ability to synchronize to an external signal [8,9]. Indeed, these theoretical and experimental studies emphasize the importance of their nonlinear character on their microwave properties. More recently, several studies have also revealed the potential strong influence of mode coupling on the nonlinearities of STNOs [10–15]. A direct consequence is that mode coupling should now be considered as a strategy to tune their intrinsic nonlinearities [16]. A reduction of nonlinearities can lead to a cancellation of the undesired linewidth broadening but concurrently to a decrease of the frequency tunability with current. However, contrary to uniformly magnetized STNOs, it has been highlighted that the vortex case has the ability to conserve large frequency tunability with current through the Oersted field [17].

In this Letter, we aim at emphasizing the interest of spin-transfer oscillators based on the current-induced dynamics of two weakly coupled vortices. In such a system, spin transfer gives rise to self-sustained oscillations of hybridized gyrotropic modes, each of them depending on the relative configuration of each vortex (core polarity and chirality). Combining experiments, analytics, and numerical simulations, we investigate the impact of relative vortex core configurations on the properties of coupled modes. We report not only the effect of core polarities on mode frequency and gyration radii but also on the evolution of the critical current and the linewidth broadening through a modification of the nonlinear parameters. Notably, we demonstrate that a strong reduction of the nonlinearities through an increase of the effective damping term can be achieved by choosing properly the coupled mode that is excited. Thus, coupled vortices appear to be a model system [18,19] for the study and the improvement of the properties of spin-transfer nano-oscillators through collective mode dynamics.

The studied samples are nanopillars with a nominal 300-nm radius made from a multilayer stack containing an in-plane magnetized CoFe/Ru/CoFeB synthetic antiferromagnet (SAFM), a MgO barrier, and then a NiFe(20 nm)/Cu(9 nm)/NiFe(8 nm) spin valve [Fig. 1(a)]. Each NiFe layer has a vortex magnetic configuration. Given that the total thickness is much larger than for a standard magnetic tunnel junction (MTJ), the etching process during the nanofabrication results in a conic shape pillar with a 290-nm radius for the top thin NiFe layer and 340-nm radius for the bottom thick layer.

In such a configuration with two vortices (2V), the existence of dipolar coupling between the two vortices

*Corresponding author.
vincent.cros@thalesgroup.com

implies that the two gyrotropic modes associated to each vortex will hybridize [20]. Each of these two coupled modes being predominantly associated to one of the vortices, the one that will be effectively excited by spin torque depends on the sign of the injected current. In our system, every combination of chiralities and core polarities can be obtained by careful magnetic preparation. However, in the following, we focus on the configuration with identical vortex chiralities, both parallel to the Oersted field. For this case, the spin-transfer dynamics of the coupled modes measured for identical (Pc) and opposite (APc) relative core polarity configurations are compared under a negative dc current (electrons flowing from the top thin-layer vortex to the bottom thick-layer vortex). It should be noted that the tunneling magnetoresistance ratio is about 70% compared to a giant magnetoresistance ratio of 3% in the spin-valve part. Therefore, the coupled mode motion (and thus the emitted power) is essentially detected through the vortex dynamics in the 20-nm-thick NiFe layer adjacent to the MgO barrier layer. For this configuration, it is anticipated that the spin-transfer torque excites the coupled mode driven by the thin-layer vortex that is in the top thin layer [21,22]. This mode has a lower frequency than the second coupled gyrotropic mode mainly associated to the thick-layer vortex which is damped by spin transfer. Thus, for both relative configurations, spin-transfer oscillations of the coupled vortex system are generated through the hybridized mode dominated by the thin layer.

Indeed, as shown in the insets in Figs. 1(b) and 1(c), for both cases a peak having a large amplitude and a narrow linewidth at a frequency close to the predicted gyrotropic frequency is detected for the isolated thin-layer vortex (197 MHz). A much broader peak (linewidth above 4 MHz) at higher frequency which is attributed to thermal excitation of the second coupled mode is also recorded. The frequency evolution of these two modes as a function of the perpendicular applied field H_z is given in Fig. 1(c) [respectively, Fig. 1(b)] for parallel (Pc) [respectively, antiparallel (APc)] relative vortex core polarities. As expected [23], the slopes of these modes have the same (respectively, opposite) sign for parallel (respectively, antiparallel) core polarities. It should be noted that the best spectral coherence for the excited mode is obtained in the APc configuration, with a minimum linewidth of 80 kHz (at $H_z = 30$ kA/m and $I_{dc} = -16$ mA) leading to a Q factor of 2400 compared to a $Q_{max} = 300$ in the Pc configuration.

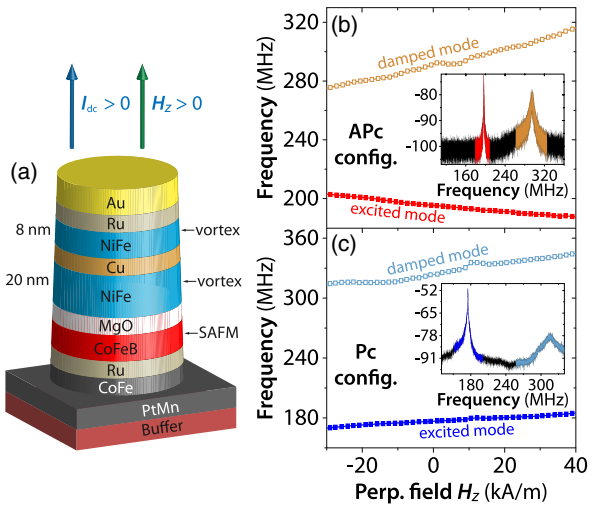

FIG. 1. (a) Schematic of an hybrid magnetic tunnel junction: a Cu-based spin-valve system with the two-vortex Py layer (8 nm at the top, 20 nm at the bottom) above a 1-nm MgO barrier and a CoFeB-based synthetic antiferromagnet. (b),(c) Field dependence of the low-frequency "excited" mode and the high-frequency "damped" mode for the APc (b) and Pc (c) configuration at $I_{dc} = -16$ mA. Inset: Frequency spectrum of the output emitted signal at $H_z = 0$ kA/m for the APc (b) and Pc (c) configuration.

The evolution with the dc current I_{dc} of both the frequency and the integrated power of the excited low-frequency mode is shown in Figs. 2(a) and 2(b) for both Pc and APc core configurations at zero applied magnetic field. Several important features can be highlighted. First, an almost strictly linear dependence of the frequency with I_{dc} is found and thus represents an interesting feature for frequency modulation using STNOs. Moreover, the two df/dI_{dc} slopes are identical and are separated by a constant frequency difference of 20 MHz. Second, the output emitted power of the excited mode is about 10 times smaller in the APc core configuration (10 nW) compared to the Pc case (100 nW). Third, the threshold current I_{cr} is found to be much lower in the APc configuration ($I_{cr}^{APc} = -12$ mA and $I_{cr}^{Pc} = -15.6$ mA).

To elucidate these large differences of microwave features of the excited modes in the two core configurations, an analytical model based on the Thiele formalism [24] has been developed. In order to describe our system, a coupling term accounting for the dipolar interaction between the two in-plane mean magnetizations of the moving vortices

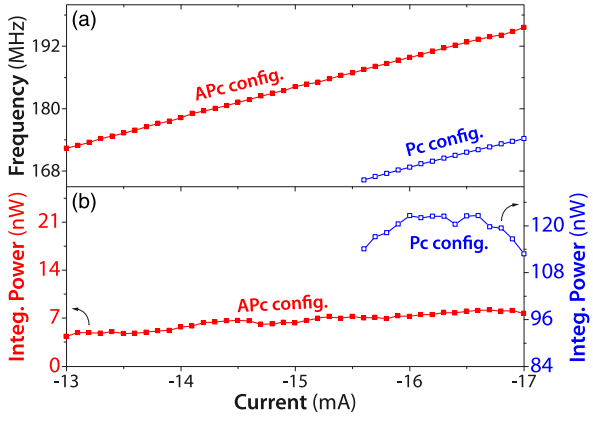

FIG. 2. Frequency (a) and integrated output emitted power (b) current dependency for the APc (red dot) and Pc (blue dot) configurations at zero applied field.

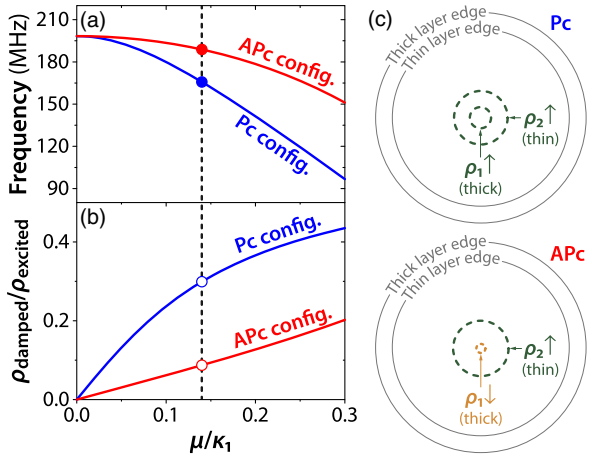

FIG. 3. Frequency vs coupling for the lowest excited mode in the parallel core (blue line) and antiparallel core (red line) for $I_{dc} = -16$ mA at zero field. (b) The ratio of gyration radii between thin and thick layers for the lowest frequency mode in the parallel (blue line) and antiparallel (red line) configurations. [Filled (unfilled) circles represent the (expected) experimental points.] (c) Micromagnetic simulations representing gyration radii (ρ_1, ρ_2) for the Pc and APc configurations at zero field, $I_{dc} = -16$ mA, and 0 K. Dot edges (black lines) present a 50-nm difference due to ion etching [see Fig. 1(a)].

(so-called body-body interaction) is added. The dipolar core-core interactions are neglected, given that the two cores are far from each other when they are moving under the action of the spin-transfer torque. In complex coordinates $\boldsymbol{X} \equiv Xe^{i\theta}$, we obtain the following system of coupled equations:

$$\frac{d\boldsymbol{X}_1}{dt} - \frac{\kappa_1(J_1)}{(ip_1G_1 - D_1)}\boldsymbol{X}_1 - \frac{\mu}{(ip_1G_1 - D_1)}\boldsymbol{X}_2 = 0,$$
$$\frac{d\boldsymbol{X}_2}{dt} - \frac{\kappa_2(J_2)}{(ip_2G_2 - D_2)}\boldsymbol{X}_2 - \frac{\mu}{(ip_2G_2 - D_2)}\boldsymbol{X}_1 = 0$$

with $\kappa_{1,2}(J_{1,2})$ the magnetostatic and Oersted field confinement coefficient [25], $p_{1,2}$ the vortex core polarity, $J_{1,2}$ the current density, $p_{1,2}G_{1,2}$ the gyrovector, $D_{1,2}$ the dyadic damping term [25], and μ the dipolar body-body coupling term. The index 1 (respectively, 2) stands for the thick- (respectively, thin-) layer vortex. It can be recalled that the sense of gyration of a vortex core depends on the core polarization through the gyrovector.

By analytically solving the system [26], we obtain for each relative configuration two eigenvalues $\lambda_{a,b}$ and two eigenvectors $\boldsymbol{V_{a,b}}$. Hence, we can extract the hybridized resonant mode frequencies $\mathrm{Im}(\lambda_{a,b})$ as well as the ratio of gyration radii in each layer $(\rho_1/\rho_2)_{a,b} = (V_{a,b})_{X_1}/(V_{a,b})_{X_2}$ with $(V_{a,b})_{X_{1,2}}$ the projection of the eigenvectors in the basis $(\boldsymbol{X}_1, \boldsymbol{X}_2)$. Note that, at this stage, neither the spin-transfer torque nor the nonlinear contribution of the confining force and the damping force are taken into account.

In Fig. 3, we display the evolution of the frequency [Fig. 3(a)] and the ratio of vortices radii [Fig. 3(b)] of the low-frequency mode as a function of the coupling strength normalized to the confinement μ/κ_1 for the Pc core configuration (blue line) and for the APc one (red line). These analytical predictions are compared to micromagnetic simulations [shown in Fig. 3(c)] including the spin-transfer torque as well as the Oersted field for which an excellent overall agreement is obtained.

From the 20-MHz frequency difference between the two core configurations found experimentally, we can estimate the matching value of the coupling coefficient [see the dotted line in Figs. 3(a) and 3(b)] to equal $\mu = 0.14\kappa_1$. Hence, we estimate the corresponding gyration radii ratio from Fig. 4(b): $\rho_1/\rho_2 = 0.3$ for identical polarities and $\rho_1/\rho_2 = 0.1$ for opposite polarities. These latter predictions for the ratio of the gyrotropic radius for each vortex are confirmed by micromagnetic simulations [Fig. 3(c) for $I_{dc} = -16$ mA, zero field, and 0 K] [27]. Indeed, we find similar radii for the gyrotropic motion of the thin-layer vortex [about 90 nm as shown in Fig. 3(c)] for both core configurations, whereas the radius of the thick-layer vortex motion strongly depends on the core configuration: 9 nm in APc and 32 nm in Pc. Finally, it has to be noticed that, even when vortices have opposite core polarities, the two vortex cores are gyrating in the same direction, confirming that the spin-transfer torque excites a single coupled mode and not two independent gyrotropic motions.

Indeed, the difference of gyration amplitude of the thin and thick vortex layers shown in Fig. 3(b) allows explaining, even quantitatively, the large difference of emitted power found experimentally between the Pc and APc core configurations [see Fig. 2(b)]: 100 nW/10 nW $\propto (\rho_{1,\mathrm{Pc}}/\rho_{1,\mathrm{APc}})^2$ [3]. In fact, this large difference of amplitude motion in the thick layer cannot be attributed to the influence of the spin transfer (as it is not taken into account in the analytical model) but rather to the sense of gyration of the vortex thick layer that is opposite to its normal one in the APc configuration [20].

To tackle the issue of the observed different spectral coherences related to the dynamical properties of these coupled modes, it is anticipated that the nonlinear character of spin-transfer oscillators should play a crucial role. Indeed, several approaches have been proposed to evaluate the influence of nonlinearities on the STNO linewidth [4,11,28,29]. Notably, it is demonstrated that the normalized dimensionless nonlinear frequency shift ν implies a conversion of amplitude fluctuations into undesired phase fluctuations. It has been proposed recently that this important parameter can be extracted through the analysis of the signal harmonics linewidths [30].

In Fig. 4, we present the evolution of the linewidth of the low-frequency coupled mode and its first harmonics [measured but out of the frequency range of Figs. 1(b) and 1(c)] as a function of I_{dc}. In the APc core configuration

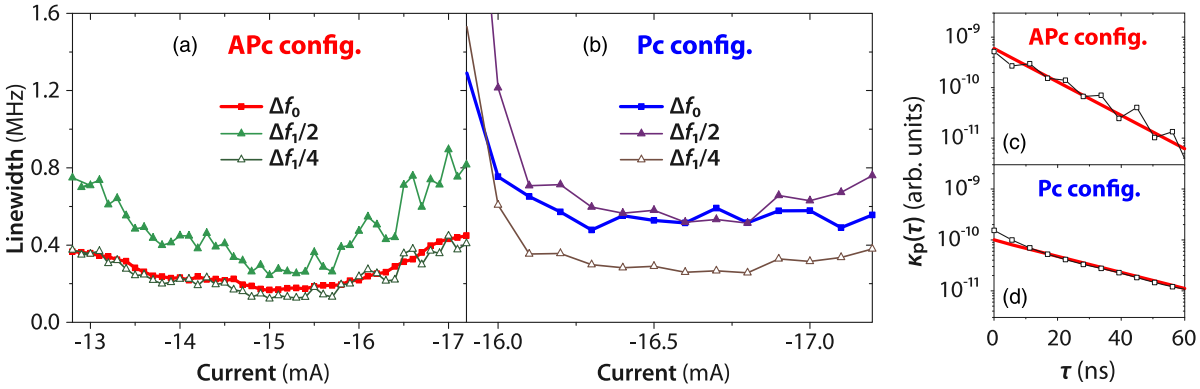

FIG. 4. Spectral linewidth of the fundamental and the first harmonics divided by two (filled symbols) and four (open symbols) for the APc (a) and Pc (b) configuration measured at zero applied magnetic field. The autocorrelation function of power fluctuations for both configurations APc (c) and Pc (d) at zero field for $I_{dc} = -17$ mA.

[Fig. 4(a)], we find that the ratio between the linewidth of the fundamental mode Δf_0 and the first harmonic Δf_1 is close to 4 in all ranges of injected current. Such behavior is consistent with an oscillator that is quasi-isochronous ($\nu \ll 1$), for which it has been predicted the linewidth of the nth harmonic to be equal to $\Delta f_n/\Delta f_0 = (n+1)^2$. This behavior strongly differs for the Pc configuration [Fig. 4(b)], for which we find a ratio close to 2 between Δf_0 and Δf_1 for all I_{dc}. This corresponds to a nonisochronous oscillator (large ν), a case for which $\Delta f_n/\Delta f_0 = (n+1)$.

This latter case obtained for the Pc core configuration appears to be similar to the single-vortex case in which a large normalized dimensionless nonlinear frequency shift ν is found [31,32]. Moreover, the strong reduction of nonlinearity in the APc configuration strongly is consistent with the much smaller linewidth (about 100 kHz) we find in the APc configuration. Indeed, linewidth broadening is directly correlated to the nonlinear behavior of the oscillator [4]. At last, we emphasize that these features are reproduced for several other samples and are also consistent with our previous studies in spin-valve nanopillars for the APc configuration [33].

The normalized dimensionless nonlinear frequency shift ν is expressed as $\nu = Np/\Gamma_p$, where N is the nonlinear frequency shift, p is the normalized oscillation power (note that this power is related to the motion of both thick- and thin-layer vortices, while the detected emitted power corresponds only to the thick-layer vortex gyration), and Γ_p is the effective damping rate that describes how fast an oscillator returns to its stable trajectory after a deviation of its amplitude. The parameter N can be estimated experimentally from the evolution of the frequency with I_{dc}: $f = f_0(I) + 2\pi N p^2$. The fact that we find similar df/dI_{dc} for both core configurations suggests that the nonlinear frequency shift N is indeed small and in any case of comparable amplitude. Then the normalized power p can be easily estimated from micromagnetic simulations. Moreover, we estimate that the normalized oscillation power is slightly higher in the Pc configuration (about 12% higher) than in the APc case. This slight difference of normalized radii compared to the reported output emitted powers is due to the fact that, in both cases, the gyration radius in the excited thin layer is much larger than in the thick one and is around 90 nm.

The last term entering in the expression of nonlinear frequency shift ν is the effective damping rate Γ_p. This parameter can be extracted from the experiments through the study of the temporal evolution of the signal. To do so, we perform Hilbert transforms on 5-ms time traces and fit the autocorrelation function of power fluctuations [as shown in Figs. 4(c) and 4(d)] with the following expression [34]:

$$\kappa_p = \langle \delta p(\tau) | \delta p(0) \rangle = A(p_0, \Gamma_p e^{-2\Gamma_p|\tau|}).$$

Through such analysis, we find that Γ_p is twice larger in the APc configuration (approximately 30 MHz) than in the Pc case (< 13 MHz). Finally, taking into account all the contributions, we deduce that the nonlinear frequency shift ν is about 3 times larger in the Pc core configuration than in APc. It is, however, to be emphasized that this "small" difference leads to drastically different microwave features, thus demonstrating the importance of tuning precisely the nonlinear parameters in these spin-transfer oscillators. An interesting feature of our coupled vortex oscillators is the factor of 2 difference on the effective damping rate Γ_p that could be of a great interest for rf applications, as it is directly linked to the modulation bandwidth [3].

In conclusion, we evidence the strong influence of vortex core configurations on the dynamics of the collective modes of the oscillator (frequency, spectral coherence, and critical current). In particular, we show the strong correlation between the vortex core configuration and the nonlinear frequency shift of the excited mode ν, a crucial parameter for describing the main rf features of the microwave signal. Indeed, we demonstrate that the

significant reduction of the linewidth broadening due to nonlinearities observed for APc is due to an increase of the effective damping parameter Γ_p. These results highlight the potential of coupled modes for potential radio-frequency, storage, or associative memories applications.

The authors acknowledge E. Grimaldi and A. Jenkins for fruitful discussions, Y. Nagamine, H. Maehara, and K. Tsunekawa of CANON ANELVA for preparing the MTJ films, and the financial support from the Agence Nationale de la Recherche (SPINNOVA ANR-11-NANO-0016) and an EU FP7 grant (MOSAIC No. ICT-FP7-n.317950). F. A. A. acknowledges the Research Science Foundation of Belgium (FRS-FNRS) for financial support (FRIA grant).

[1] Nicolas Locatelli, Vincent Cros, and Julie Grollier, Spin-torque building blocks, Nat. Mater. **13**, 11 (2014).

[2] Mark D. Stiles and Jacques Miltat, in *Spin Dynamics in Confined Magnetic Structures III*, Vol. 101, edited by Burkard Hillebrands and André Thiaville (Springer, Berlin, 2006), pp. 225–308.

[3] Andrei N. Slavin and Vasil S. Tiberkevich, Nonlinear auto-oscillator theory of microwave generation by spin-polarized current, IEEE Trans. Magn. **45**, 1875 (2009).

[4] Joo-Von Kim, Vasil S. Tiberkevich, and Andrei N. Slavin, Generation linewidth of an auto-oscillator with a nonlinear frequency shift: Spin-torque nano-oscillator, Phys. Rev. Lett. **100**, 017207 (2008).

[5] Mark W. Keller, M. R. Pufall, W. H. Rippard, and T. J. Silva, Nonwhite frequency noise in spin torque oscillators and its effect on spectral linewidth, Phys. Rev. B **82**, 054416 (2010).

[6] S. Y. Martin, C. Thirion, C. Hoarau, C. Baraduc, and B. Diény, Tunability versus deviation sensitivity in a nonlinear vortex oscillator, Phys. Rev. B **88**, 024421 (2013).

[7] Ezio Iacocca and Johan Åkerman, Analytical investigation of modulated spin-torque oscillators in the framework of coupled differential equations with variable coefficients, Phys. Rev. B **85**, 184420 (2012).

[8] Benoit Georges, Julie Grollier, Michaël Darques, Vincent Cros, Cyrile Deranlot, B. Marcilhac, G. Faini, and Albert Fert, Coupling efficiency for phase locking of a spin transfer nano-oscillator to a microwave current, Phys. Rev. Lett. **101**, 017201 (2008).

[9] V. E. Demidov, H. Ulrichs, S. V. Gurevich, S. O. Demokritov, V. S. Tiberkevich, A. N. Slavin, A. Zholud, and S. Urazhdin, Synchronization of spin hall nano-oscillators to external microwave signals, Nat. Commun. **5**, 3179 (2014).

[10] J. C. Sankey, I. N. Krivorotov, S. I. Kiselev, P. M. Braganca, N. C. Emley, R. A. Buhrman, and D. C. Ralph, Mechanisms limiting the coherence time of spontaneous magnetic oscillations driven by dc spin-polarized currents, Phys. Rev. B **72**, 224427 (2005).

[11] Ezio Iacocca, Olle Heinonen, P. K. Muduli, and Johan Åkerman, Generation linewidth of mode-hopping spin torque oscillators, Phys. Rev. B **89**, 054402 (2014).

[12] I. N. Krivorotov, N. C. Emley, R. A. Buhrman, and D. C. Ralph, Time-domain studies of very-large-angle magnetization dynamics excited by spin transfer torques, Phys. Rev. B **77**, 054440 (2008).

[13] Alina M. Deac, Akio Fukushima, Hitoshi Kubota, Hiroki Maehara, Yoshishige Suzuki, Shinji Yuasa, Yoshinori Nagamine, Koji Tsunekawa, David D. Djayaprawira, and Naoki Watanabe, Bias-driven high-power microwave emission from mgo-based tunnel magnetoresistance devices, Nat. Phys. **4**, 803 (2008).

[14] S. S. Cherepov, B. C. Koop, A. Yu. Galkin, R. S. Khymyn, B. A. Ivanov, D. C. Worledge, and V. Korenivski, Core-core dynamics in spin vortex pairs, Phys. Rev. Lett. **109**, 097204 (2012).

[15] J. F. Pulecio, P. Warnicke, S. D. Pollard, D. A. Arena, and Y. Zhu, Coherence and modality of driven interlayer-coupled magnetic vortices, Nat. Commun. **5**, 3760 (2014).

[16] D. Gusakova, M. Quinsat, J. F. Sierra, U. Ebels, B. Dieny, L. D. Buda-Prejbeanu, M.-C. Cyrille, V. Tiberkevich, and A. N. Slavin, Linewidth reduction in a spin-torque nano-oscillator caused by non-conservative current-induced coupling between magnetic layers, Appl. Phys. Lett. **99**, 052501 (2011).

[17] V. S. Pribiag, I. N. Krivorotov, G. D. Fuchs, P. M. Braganca, O. Ozatay, J. C. Sankey, D. C. Ralph, and R. A. Buhrman, Magnetic vortex oscillator driven by d.c. spin-polarized current, Nat. Phys. **3**, 498 (2007).

[18] Nicolas Locatelli, V. V. Naletov, Julie Grollier, Grégoire De Loubens, Vincent Cros, Cyrile Deranlot, C. Ulysse, G. Faini, Olivier Klein, and Albert Fert, Dynamics of two coupled vortices in a spin valve nanopillar excited by spin transfer torque, Appl. Phys. Lett. **98**, 062501 (2011).

[19] F. Abreu Araujo, M. Darques, K. A. Zvezdin, A. V. Khvalkovskiy, N. Locatelli, K. Bouzehouane, V. Cros, and L. Piraux, Microwave signal emission in spin-torque vortex oscillators in metallic nanowires: Experimental measurements and micromagnetic numerical study, Phys. Rev. B **86**, 064424 (2012).

[20] K. Y. Guslienko, B. A. Ivanov, V. Novosad, Y. Otani, H. Shima, and K. Fukamichi, Eigenfrequencies of vortex state excitations in magnetic submicron-size disks, J. Appl. Phys. **91**, 8037 (2002).

[21] A. V. Khvalkovskiy, J. Grollier, N. Locatelli, Y. V. Gorbunov, K. A. Zvezdin, and V. Cros, Nonuniformity of a planar polarizer for spin-transfer-induced vortex oscillations at zero field, Appl. Phys. Lett. **96**, 212507 (2010).

[22] These measurements are performed at zero or small applied perpendicular magnetic field, allowing us to neglect additional contributions to spin torque arising from the SAFM of the MTJ [21].

[23] Grégoire de Loubens, A. Riegler, Benjamin Pigeau, F. Lochner, F. Boust, Konstantin Yu. Guslienko, H. Hurdequint, L. W. Molenkamp, G. Schmidt, Andrei N. Slavin, Vasil S. Tiberkevich, N. Vukadinovic, and Olivier Klein, Bistability of vortex core dynamics in a single perpendicularly magnetized nanodisk, Phys. Rev. Lett. **102**, 177602 (2009).

[24] K. Yu. Guslienko, K. S. Buchanan, S. D. Bader, and V. Novosad, Dynamics of coupled vortices in layered magnetic nanodots, Appl. Phys. Lett. **86**, 223112 (2005).

[25] A. Dussaux, A. V. Khvalkovskiy, P. Bortolotti, J. Grollier, V. Cros, and A. Fert, Field dependence of spin-transfer-induced vortex dynamics in the nonlinear regime, Phys. Rev. B **86**, 014402 (2012).

[26] We use the parameters (thickness and diameter) corresponding to our systems with a NiFe magnetization, $M_s = 600$ emu cm^{-3} and $\alpha = 0.01$.

[27] See Supplemental Material at for analytical verification at http://link.aps.org/supplemental/10.1103/PhysRevApplied.2.061001 for analytical verification at other values of current or through the frequencies of the high-frequency damped mode.

[28] Graham E. Rowlands, Jordan A. Katine, Juergen Langer, Jian Zhu, and Ilya N. Krivorotov, Time domain mapping of spin torque oscillator effective energy, Phys. Rev. Lett. **111**, 087206 (2013).

[29] O. J. Lee, P. M. Braganca, V. S. Pribiag, D. C. Ralph, and R. A. Buhrman, Quasilinear spin-torque nano-oscillator via enhanced negative feedback of power fluctuations, Phys. Rev. B **88**, 224411 (2013).

[30] M. Quinsat, V. Tiberkevich, D. Gusakova, A. Slavin, J. F. Sierra, U. Ebels, L. D. Buda-Prejbeanu, B. Dieny, M.-C. Cyrille, A. Zelster, and J. A. Katine, Linewidth of higher harmonics in a nonisochronous auto-oscillator: Application to spin-torque nano-oscillators, Phys. Rev. B **86**, 104418 (2012).

[31] Eva Grimaldi, Antoine Dussaux, Paolo Bortolotti, Julie Grollier, Grégoire Pillet, Akio Fukushima, Hitoshi Kubota, Kay Yakushiji, Shinji Yuasa, and Vincent Cros, Response to noise of a vortex based spin transfer nano-oscillator, Phys. Rev. B **89**, 104404 (2014).

[32] F. Sanches, V. Tiberkevich, K. Y. Guslienko, J. Sinha, M. Hayashi, O. Prokopenko, and A. N. Slavin, Current-driven gyrotropic mode of a magnetic vortex as a nonisochronous auto-oscillator, Phys. Rev. B **89**, 140410 (2014).

[33] A. Hamadeh, N. Locatelli, V. V. Naletov, R. Lebrun, G. de Loubens, J. Grollier, O. Klein, and V. Cros, Origin of spectral purity and tuning sensitivity in a spin transfer vortex nano-oscillator, Phys. Rev. Lett. **112**, 257201 (2014).

[34] L. Bianchini, S. Cornelissen, Joo-Von Kim, T. Devolder, W. van Roy, L. Lagae, and C. Chappert, Direct experimental measurement of phase-amplitude coupling in spin torque oscillators, Appl. Phys. Lett. **97**, 032502 (2010).